Photoelectrochemical Behavior of n-Type Si(111) Electrodes Coated With a Single Layer of Graphene

Adam C. Nielander,[†] Matthew J. Bierman,[†,§] Nicholas Petrone,[‡] Nicholas C. Strandwitz,[†,∥] Shane Ardo,[†] Fan Yang,[†] James Hone,*[‡] and Nathan S. Lewis*[†]

[†]Division of Chemistry and Chemical Engineering, California Institute of Technology, Pasadena, California 91125, United States
[‡]Department of Mechanical Engineering, Columbia University, New York, New York 10027, United States

S Supporting Information

ABSTRACT: The behavior of graphene-coated n-type Si(111) photoanodes was compared to the behavior of H-terminated n-type Si(111) photoanodes in contact with aqueous $K_3[Fe(CN)_6]/K_4[Fe(CN)_6]$ as well as in contact with a series of outer-sphere, one-electron redox couples in nonaqueous electrolytes. The n-Si/Graphene electrodes exhibited stable short-circuit photocurrent densities of over 10 mA cm^{-2} for >1000 s of continuous operation in aqueous electrolytes, whereas n-Si−H electrodes yielded a nearly complete decay of the current density within ~100 s. The values of the open-circuit photovoltages and the flat-band potentials of the Si were a function of both the Fermi level of the graphene and the electrochemical potential of the electrolyte solution, indicating that the n-Si/Graphene did not form a buried junction with respect to the solution contact.

Various strategies have been developed to stabilize photoanodes such as n-Si against photocorrosion or photopassivation in aqueous electrolytes. Thin overlayers of metal have yielded improved anodic stability for silicon and other semiconductors, but generally form semiconductor/metal Schottky barriers that pin the Fermi level of the semiconductor, producing nonoptimal photovoltages.[1−7] Furthermore, nearly complete protection from degradation generally requires the deposition of relatively thick metal layers, preventing a significant fraction of incident light from reaching the underlying semiconductor. Insulating barrier layers, such as oxides deposited by atomic layer deposition, or oxides formed via electrochemical anodization processes, can also provide some degree of protection against corrosion.[8−10] However, these oxides generally require deposition of pinhole-free films that form a tunneling barrier to photogenerated holes, in many cases producing a significant series resistance that negatively affects the performance of the resulting photoelectrochemical device. Surface functionalization has led to improvements in the stability of n-Si photoanodes in H_2O-containing nonaqueous solvents, but surface-modification approaches have not yet yielded materials that remain stable under extended anodic operation in aqueous electrolytes.[11−13]

Graphene has the potential to be an almost ideal protection layer for semiconductor photoelectrodes. Graphene can be prepared in nearly pinhole-free large-area layers and has been shown to attenuate the oxidation of metals in air as well as in aqueous electrochemical environments.[14−19] Unlike surface functionalization techniques that are typically specific to a semiconductor and surface plane, graphene layers can be readily applied to a variety of planar electrode surfaces. Graphene also has excellent optical properties, exhibiting ~97% transmission in the visible region of the solar spectrum.[20] Further, graphene has been used in solid-state Schottky junctions capable of generating photocurrent.[21,22] The high carrier mobility in the plane of the graphene C−C bonds should allow for lateral transport of carriers to catalytically active sites on the surface of the photoelectrode.[23] The low density of states near the Fermi level of graphene, the chemical inertness of graphene, and the ability to deposit graphene at room temperature and thereby avoid high-temperature interfacial reactions potentially provide an opportunity to deposit conductive graphene monolayers onto a variety of semiconductor photoanodes, while obtaining desirable photoelectrochemical performance from the resulting solid/liquid junctions.[14,24,25]

Accordingly, graphene-covered n-Si (n-Si/Gr) electrodes were fabricated by floating graphene that had been grown using chemical vapor deposition (CVD) onto H-terminated n-Si(111) surfaces. X-ray photoelectron spectroscopic (XPS) analysis indicated that this fabrication technique resulted in an intervening 1−2 monolayer thick oxide layer between the silicon and graphene (see Supporting Information (SI)).

Figure 1a depicts the current density vs potential ($J−E$) behavior in the presence and absence of illumination of n-Si/Gr and n-Si−H electrodes in contact with CH_3CN−5 mM ferrocenium (Fc^+)−50 mM ferrocene (Fc^0)−1.0 M LiClO$_4$. The open-circuit photovoltage, V_{oc}, was 310 mV for Si−H surfaces and was 260 mV for the n-Si/Gr electrodes. The n-Si/Gr electrodes showed somewhat smaller fill factors (ff) than the n-Si−H electrodes (0.40 vs 0.64), indicating the presence of a resistance at the n-Si/Gr/CH_3CN contact.

After five potential sweeps in contact with 50 mM $Fe(CN)_6^{3-}$−350 mM $Fe(CN)_6^{4-}$(aq), the n-Si−H electrode exhibited negligible photocurrent over the power-producing potential range, consistent with expectations for the formation of an insulating oxide layer under photoanodic conditions.[11] In contrast, the n-Si/Gr photoelectrode exhibited essentially no change in $J−E$ behavior under the same conditions, with V_{oc} = 340 mV and ff = 0.30 (Figure 1b). As shown in Figure 1c, after
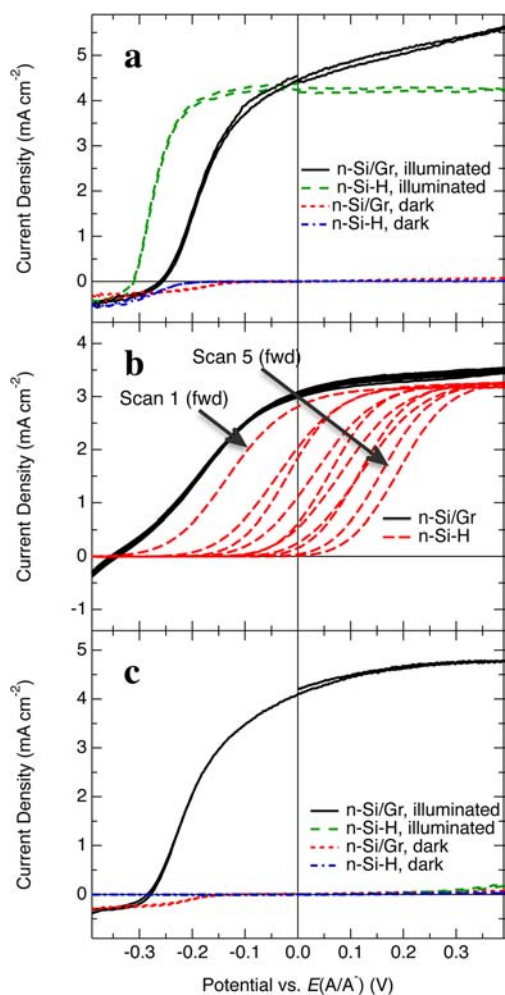
Figure 1. (a) *J*−*E* behavior of freshly fabricated n-Si/Gr and n-Si−H electrodes in contact with CH_3CN−$Fc^{+/0}$ under illumination and in the dark. (b) *J*−*E* behavior (5 cycles at 30 mV s^{-1}) of the n-Si/Gr and n-Si−H electrodes from (a) in $Fe(CN)_6^{3-/4-}$(aq) under illumination. The first forward (fwd) scan and fifth forward scan are labeled with arrows. (c) *J*−*E* behavior (1 cycle) of the n-Si/Gr and n-Si−H electrodes in CH_3CN−$Fc^{+/0}$ in the presence and absence of illumination, after the data collection depicted in (b).

Figure 2. (a) Comparison of the *J*−*t* behavior of potentiostatically controlled n-Si/Gr and n-Si−H electrodes (*E* = 0 V vs the solution) in contact with $Fe(CN)_6^{3-/4-}$(aq) under illumination required to produce a short-circuit photocurrent density of ∼11 mA cm^{-2} (∼33 mW/cm^2). The illumination began at *t* = 10 s. (b) *J*−*t* behavior of an n-Si/Gr electrode in $Fe(CN)_6^{3-/4-}$(aq) under illumination required to produce a short-circuit photocurrent density of ∼11 mA cm^{-2} over 1000 s (*E* = 0 V vs the solution). The slight increase in current over 1000 s was attributed to instability in the light source.

photoelectrochemical operation in contact with $Fe(CN)_6^{3-/4-}$ (aq), the *J*−*E* behavior of the n-Si/Gr photoanode in contact with the CH_3CN−$Fc^{+/0}$ redox system was almost unchanged from its initial properties in this electrolyte. In fact, a minor improvement in V_{oc} was observed, as well as an apparent decrease in the parallel shunt resistance as indicated by the decreased dependence of the current on applied potential under reverse bias. This is consistent with the passivation of shunts via oxidation in aqueous solution. The chemical nature of these shunts may be due to trace metal impurities from the fabrication procedure or 'dangling' Si bonds present due to the formation of a nonstoichiometric silicon oxide.

Figure 2 further displays the stability toward photo-passivation of the n-Si/Gr surface relative to the n-Si−H surface. Both the n-Si/Gr and the n-Si−H electrodes were immersed in $Fe(CN)_6^{3-/4-}$(aq) and illuminated to produce ∼11 mA cm^{-2} of photocurrent at a potential of *E* = 0 V vs the Nernstian potential of the solution. The n-Si/Gr electrode exhibited stable photocurrents, whereas the n-Si−H electrode decayed back to baseline within ∼100 s (Figure 2a). Figure 2b
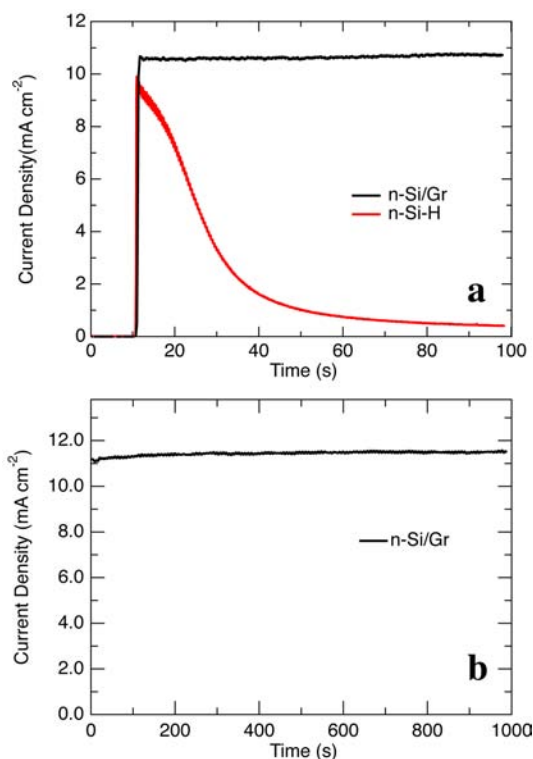
extends the experiment on the n-Si/Gr electrodes to 1000 s. Additionally, comparison of the stability in $Fe(CN)_6^{3-/4-}$(aq) of an n-Si/Gr electrode to that of methylated n-Si(111) electrodes showed that graphene was significantly more effective at preventing electrochemical performance degradation (see SI), albeit without the interfacial dipole that increases the V_{oc} of n-type CH_3−Si(111) surfaces relative to H−Si(111) surfaces. Comparison of the n-Si/Gr electrode stability in $Fe(CN)_6^{3-/4-}$(aq) to that of n-Si−H electrode stability under ∼100 mW/cm^{-2} illumination indicated degradation of both electrodes, albeit at much higher rates for the n-Si−H system (see SI).

Figure 3 compares the *J*−*E* behavior of freshly prepared n-Si/Gr electrodes in contact with CH_3CN−cobaltocene ($CoCp_2^{+/0}$) to the *J*−*E* behavior of n-Si/Gr electrodes in contact with CH_3CN−$Fc^{+/0}$ and CH_3CN−acetylferrocene ($AcFc^{+/0}$). The moderate V_{oc} observed for n-Si/Gr/CH_3CN-$Fc^{+/0}$ contacts, larger V_{oc} observed for n-Si/Gr/CH_3CN−$AcFc^{+/0}$ contacts, and negligible V_{oc} in contact with CH_3CN−$CoCp_2^{+/0}$ are in accord with the expectation of increasing V_{oc} with increasingly oxidizing electrolyte potentials and also consistent with the junction energetics being controlled at least in part by the difference in electrochemical potential between the Si and liquid phase. After operation in both electrolytes, the n-Si/Gr electrodes were then operated under photoanodic conditions in contact with $Fe(CN)_6^{3-/4-}$(aq), in an analogous fashion to the electrodes shown in Figure 1b.
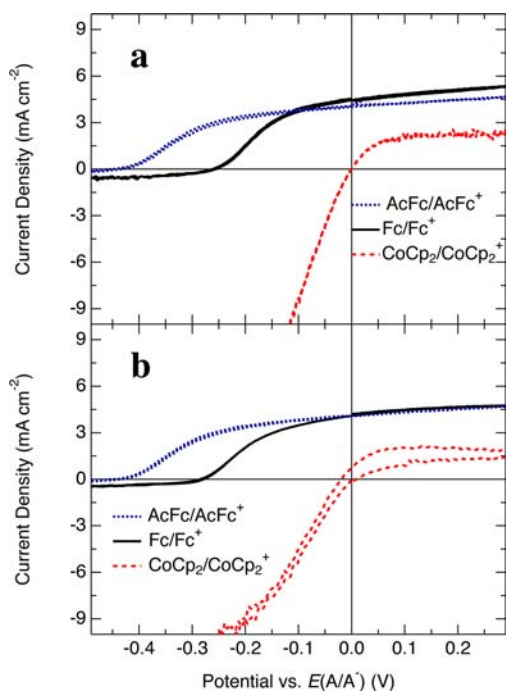
Figure 3. (a) J−E behavior (forward and reverse scan) of n-Si/Gr electrodes in CH_3CN−$AcFc^{+/0}$ (V_{oc} = 0.43 V), CH_3CN−$Fc^{+/0}$ (V_{oc} = 0.26 V), and CH_3CN−$CoCp_2^{+/0}$ (V_{oc} = 0 V) under illumination prior to exposure to $[Fe(CN)_6]^{3-/4-}$(aq). (b) J−E behavior of n-Si/Gr electrodes in CH_3CN-$AcFc^{+/0}$ (V_{oc} = 0.43 V), CH_3CN-$Fc^{+/0}$ (V_{oc} = 0.28 V), and CH_3CN-$CoCp_2^{+/0}$ (V_{oc} = 0 V) under illumination after exposure to $[Fe(CN)_6]^{3-/4-}$(aq). The solution potentials were as follows: $E(AcFc^{+/0})$ = +0.4 V vs $E^0(Fc^{+/0})$, $E(Fc^{+/0})$ = −0.1 V vs $E^0(Fc^{+/0})$, and $E(CoCp_2^{+/0})$ = −1.26 V vs $E^0(Fc^{+/0})$

The data of Figure 3b indicate that the electrochemical properties of the electrodes were essentially unaffected by operation in the oxidizing $Fe(CN)_6^{3-/4-}$(aq) environment. If pinholes in the graphene had controlled the junction energetics, the Si exposed through these pinholes would presumably have passivated upon treatment in $Fe(CN)_6^{3-/4-}$(aq), leaving only the graphene-covered regions to control the junction energetics. Thus, the measurement of V_{oc} > 200 mV for n-Si/Gr in contact with $Fc^{+/0}$, V_{oc} >400 mV for n-Si/Gr/$AcFc^{+/0}$ contacts, and negligible V_{oc} for n-Si/Gr/$CoCp_2^{+/0}$ contacts indicates that the Fermi level of the n-Si/Gr electrodes was not fully pinned by the presence of graphene at the silicon/graphene/electrolyte junction. The V_{oc} for n-Si/Gr electrodes in contact with CH_3CN−$Fc^{+/0}$ was consistently smaller than the V_{oc} of n-Si−H in contact with the same electrolyte (cf. Figure 1a). The data in Figures 1−3 were highly reproducible between electrodes.

This behavior is consistent with expectations that the limited number of electronic states in graphene affect the junction energetics without fully pinning the Fermi level of the semiconductor. Specifically, Poisson's equation was solved while treating the n-Si/Gr/electrolyte interface as consisting of a depleted semiconductor (Si) of known dielectric and capacitive properties in contact with an atomically thin material with the known density of electronic states as a function of energy of graphene, with this entire phase in contact with a phase consisting of the known dielectric and capacitive properties representative of a typical electrolyte solution. An initial difference in Fermi levels of ∼0.8 eV between the semiconductor and the electrolyte should produce a maximum potential drop of ∼0.65 V in the Si space-charge region, with the remainder dropping across the solid/liquid interface. Mott−Schottky ($1/C^2$ vs E) data yielded support for this model, in that a lower barrier height was observed for the n-Si/Gr/CH_3CN−$Fc^{+/0}$ contacts than for n-Si−H/CH_3CN/$Fc^{+/0}$ contacts which are expected to show a potential drop of nearly ∼0.8 V in the Si space charge region (see SI). This behavior is consistent with a portion of the total potential drop occurring in the graphene and solution layer as opposed to the space-charge region of the semiconductor and is also consistent with the smaller V_{oc} of n-Si/Gr/CH_3CN-$Fc^{+/0}$ contacts relative to n-Si−H/CH_3CN−$Fc^{+/0}$ contacts. Many factors, including the formation of a thin insulating oxide as well as changes in charge-transfer kinetics, can affect the relationship between the barrier height and V_{oc} and could account for the somewhat smaller change in V_{oc} relative to the change in barrier height.

Fitting the forward-bias dark J−E behavior of the n-Si/Gr/CH_3CN−$Fc^{+/0}$ contact to the diode equation, $J = J_0*[exp(-q\Delta V/\eta kT) - 1]$, where J_0 is the exchange current density, q is the unsigned charge on an electron, k is Boltzmann's constant, T is the absolute temperature, η is the diode quality factor, and ΔV is the difference between the applied potential and the Nernst potential of the solution, yielded $J_0 = 9.61 \times 10^{-7}$ A cm^{-2} ($\pm 6.10 \times 10^{-8}$) and η = 1.65 (± 0.02). Analysis of the dark J−E behavior of a freshly HF-etched n-Si−H electrode in contact with CH_3CN−$Fc^{+/0}$ yielded $J_0 = (6.80 \pm 0.51) \times 10^{-8}$ A cm^{-2} and η= 1.25 ± 0.012. The $J_{0,n-Si−H}$ and $J_{0,n-Si/Gr}$ values for these contacts were much smaller than the values obtained for Si/Gr/CH_3CN-$CoCp_2^{+/0}$ contacts ($J_0 \approx 10^{-3}$ A cm^{-2}) and were comparable to J_0 values reported for a highly rectifying n-Si/organic conducting polymer contact ($J_0 \approx 2 \times 10^{-8}$ A cm^{-2}). Similar to the reported results for n-Si/polymer contacts, the J_0 values for n-Si/Gr in contact with varying redox species spanned approximately 5 orders of magnitude, in comparison to n-Si/metal contacts, which are generally limited to a range of 3 orders of magnitude in J_0.[26] This further supports the conclusion that the Si/Gr/electrolyte interface was only partially pinned by the presence of graphene. The higher than unity ideality factor could result from a number of factors, including the voltage drop across the small amount of interfacial oxide as well as the voltage-dependent surface charge density that is expected from the observations and modeling of the interfacial energetics.

The ability of graphene to protect metallic electrodes against corrosion is controversial.[14−16,27] Herein we have clearly demonstrated that graphene markedly enhances the stability of silicon toward passivation by oxide formation under illumination, even in the stressing case of anodic operation in contact with aqueous solutions. In addition, we have elucidated the effects of graphene on the interfacial energetics of semiconductor/liquid contacts, which is not accessible on metallic electrodes and thus has not been defined or elucidated previously. The V_{oc} vs solution potential relationships observed from the J−E data demonstrate that Fermi-level pinning by graphene did not fully limit the observed photovoltages. Further study is required to determine whether the photovoltage is maximized for the n-Si/Gr system in contact with CH_3CN−$AcFc^{+/0}$. Extended studies of the stability imparted by graphene to silicon surfaces and the electronic and chemical effects of graphene on the silicon surface are currently underway to elucidate the extent of the graphene-imparted stability especially for bilayer and multilayer graphene coatings, as well as the effect of graphene on the surface chemistry and

recombination characteristics of the underlying Si and the effect of graphene on n-Si/oxygen-evolution catalyst systems.

ASSOCIATED CONTENT

Supporting Information

Detailed experimental procedure, analysis of graphene quality, Mott−Schottky analysis, n-Si/Gr/electrolyte phase modeling, n-Si−Me vs n-Si/Gr stability comparison, and n-Si/Gr stability under ~100 mW/cm^{-2} illumination. This material is available free of charge via the Internet at http://pubs.acs.org.

AUTHOR INFORMATION

Corresponding Authors
nslewis@caltech.edu (N.L.)
jh2228@columbia.edu (J.H.)

Present Addresses
§The Dow Chemical Company, 1776 Building, Midland, MI 48674, USA.
‖Lehigh University, Department of Materials Science and Engineering, Bethlehem, PA 18015, USA.

Notes
The authors declare no competing financial interest.

ACKNOWLEDGMENTS

REFERENCES

(1) Sze, S. M.; Ng, K. K. *Physics of Semiconductor Devices*; 3rd ed.; John Wiley & Sons, Inc.: Hoboken, NJ, 2007.
(2) Menezes, S.; Heller, A.; Miller, B. *J. Electrochem. Soc.* **1980**, *127*, 1268.
(3) Bélanger, D.; Dodelet, J. P.; Lombos, B. A. *J. Electrochem. Soc.* **1986**, *133*, 1113.
(4) Contractor, A. Q.; Bockris, J. O. M. *Electrochim. Acta* **1984**, *29*, 1427.
(5) Howe, A. T.; Hawkins, R. T.; Fleisch, T. H. *J. Electrochem. Soc.* **1986**, *133*, 1369.
(6) Fan, F. R. F.; Shea, T. V.; Bard, A. J. *J. Electrochem. Soc.* **1984**, *131*, 828.
(7) Nakato, Y.; Ueda, K.; Yano, H.; Tsubomura, H. *J. Phys. Chem.* **1988**, *92*, 2316.
(8) Strandwitz, N. C.; Comstock, D. J.; Grimm, R. L.; Nichols-Nielander, A. C.; Elam, J.; Lewis, N. S. *J. Phys. Chem. C* **2013**, *117*, 4931.
(9) Fonash, S. J. *Solar Cell Device Physics*, 2nd ed.; Elsevier Inc.: Amsterdam, 2010.
(10) Chen, Y. W.; Prange, J. D.; Dühnen, S.; Park, Y.; Gunji, M.; Chidsey, C. E. D.; McIntyre, P. C. *Nat. Mater.* **2011**, *10*, 539.
(11) Bansal, A.; Lewis, N. S. *J. Phys. Chem. B* **1998**, *102*, 4058.
(12) Bansal, A.; Lewis, N. S. *J. Phys. Chem. B* **1998**, *102*, 1067.
(13) Bolts, J. M.; Bocarsly, A. B.; Palazzotto, M. C.; Walton, E. G.; Lewis, N. S.; Wrighton, M. S. *J. Am. Chem. Soc.* **1979**, *101*, 1378.
(14) Chen, S.; Brown, L.; Levendorf, M.; Cai, W.; Ju, S.-Y.; Edgeworth, J.; Li, X.; Magnuson, C. W.; Velamakanni, A.; Piner, R. D.; Kang, J.; Park, J.; Ruoff, R. S. *ACS Nano* **2011**, *5*, 1321.
(15) Prasai, D.; Tuberquia, J. C.; Harl, R. R.; Jennings, G. K.; Bolotin, K. I. *ACS Nano* **2012**, *6*, 1102.
(16) Sutter, E.; Albrecht, P.; Camino, F. E.; Sutter, P. *Carbon* **2010**, *48*, 4414.
(17) Lee, Y.; Bae, S.; Jang, H.; Jang, S.; Zhu, S.-E.; Sim, S. H.; Song, Y. I.; Hong, B. H.; Ahn, J.-H. *Nano Lett.* **2010**, *10*, 490.
(18) Suk, J. W.; Kitt, A.; Magnuson, C. W.; Hao, Y.; Ahmed, S.; An, J.; Swan, A. K.; Goldberg, B. B.; Ruoff, R. S. *ACS Nano* **2011**, *5*, 6916.
(19) Flynn, G. W. *J. Chem. Phys.* **2011**, *135*, 050901.
(20) Mak, K. F.; Sfeir, M. Y.; Wu, Y.; Lui, C. H.; Misewich, J. A.; Heinz, T. F. *Phys. Rev. Lett.* **2008**, *101*, 196405.
(21) Li, X.; Zhu, H.; Wang, K.; Cao, A.; Wei, J.; Li, C.; Jia, Y.; Li, Z.; Li, X.; Wu, D. *Adv. Mater.* **2010**, *22*, 2743.
(22) Chen, C.-C.; Aykol, M.; Chang, C.-C.; Levi, A. F. J.; Cronin, S. B. *Nano Lett.* **2011**, *11*, 1863.
(23) Morozov, S. V.; Novoselov, K. S.; Katsnelson, M. I.; Schedin, F.; Elias, D. C.; Jaszczak, J. A.; Geim, A. K. *Phys. Rev. Lett.* **2008**, *100*, 016602.
(24) Droscher, S.; Roulleau, P.; Molitor, F.; Studerus, P.; Stampfer, C.; Ensslin, K.; Ihn, T. *Appl. Phys. Lett.* **2010**, *96*, 152104.
(25) Ponomarenko, L. A.; Yang, R.; Gorbachev, R. V.; Blake, P.; Mayorov, A. S.; Novoselov, K. S.; Katsnelson, M. I.; Geim, A. K. *Phys. Rev. Lett.* **2010**, *105*, 136801.
(26) Sailor, M. J.; Klavetter, F. L.; Grubbs, R. H.; Lewis, N. S. *Nature* **1990**, *346*, 155.
(27) Schriver, M.; Regan, W.; Gannett, W. J.; Zaniewski, A. M.; Crommie, M. F.; Zettl, A. *ACS Nano* **2013**, *7*, 5763.